



## Accurate modeling approach for the structural comparison between monolayer polymer tubes and single-walled nanotubes


Thomas Vogel<sup>a,b,\*</sup>, Tali Mutat<sup>c</sup>, Joan Adler<sup>c</sup>, Michael Bachmann<sup>a,b</sup>

<sup>a</sup>Soft Matter Systems Research Group, Institut für Festkörperforschung (IFF-2), Forschungszentrum Jülich, D-52425 Jülich, Germany

<sup>b</sup>Center for Simulational Physics, Department of Physics and Astronomy, The University of Georgia, Athens, GA, 30602, USA

<sup>c</sup>Department of Physics, Technion, Israel Institute of Technology, Haifa, 32000, Israel

data, citation and similar papers at [core.ac.uk](http://core.ac.uk)

brought to you by  CORE

provided by Elsevier - Publisher Connector

### Abstract

In a recent computational study, we found highly structured ground states for coarse-grained polymers adsorbed to ultrathin nanowires in a certain model parameter region. Those tubelike configurations show, even at a first glance, exciting morphological similarities to known atomistic nanotubes such as single-walled carbon nanotubes. In order to explain those similarities in a systematic way, we performed additional detailed and extensive simulations of coarse-grained polymer models with various parameter settings. We show this here and explain why standard geometrical models for atomistic nanotubes are not suited to interpret the results of those studies. In fact, the general structural behavior of polymer nanotubes, as well as specific previous observations, can only be explained by applying recently developed polyhedral tube models.

**Keywords:** polymer adsorption, geometry of carbon nanotubes, polyhedral model for boron nanotubes, Monte Carlo computer simulations

**PACS:** 82.35.Gh, 05.10.Ln, 61.48.De

### 1. Motivation

The considerations of the importance of exact geometric calculations when dealing with curved nanostructures that we now present arose from observations we made during a recent study [1–3]. There, we investigated polymers adsorbed at ultrathin nanowires by means of Monte Carlo simulations applying a common coarse-grained bead–stick model. For very high adsorption strengths we found, independently of the effective radius of the nanowire, well-ordered tubelike monolayer ground-state structures for that system. Those polymer tubes are formed by aligned helical monomer strands and possess different chiralities for different tube radii. Similar structural behavior is known from several tubelike atomic structures with applications in nanotechnology such as single walled carbon nanotubes [4–7].

In order to reveal the morphological similarities between the polymer monolayer tubes and atomic nanotubes, we first review the common geometrical view of these structures (Sect. 2). We show in Sect. 3 that these approximations are not suitable to explain our findings and how it should be corrected. Finally, we show in Sect. 4 how exact geometrical calculations of curved discrete tubes can provide the link between previous results [1] and results from additional exhaustive and detailed computational studies of ground states of polymer nanotubes and real-world atomic nanotubes [8].

\*Corresponding author. E-mail: [thomasvogel@physast.uga.edu](mailto:thomasvogel@physast.uga.edu)

URL: <http://phycomp.technion.ac.il/> (Joan Adler), <http://www.smsyslab.org/> (Michael Bachmann)

## 2. Review of the traditional approach to nanotube geometry

A common conception about single-walled carbon nanotubes is that they are 'built of' rolled up and optionally tilted graphene sheets which are carbon atoms crystallized in a monolayer honeycomb lattice, as depicted in Fig. 1. The standard geometrical description is hence based on this corresponding unzipped planar representation, which is uniquely defined by a wrapping vector  $\mathbf{C}_h$  pointing from an atomic position to its next periodic copy (see Fig. 2). This vector can be represented as a linear combination of two base vectors  $\mathbf{a}_1$  and  $\mathbf{a}_2$  and two integer numbers  $n$  and  $m$ :  $\mathbf{C}_h = n \mathbf{a}_1 + m \mathbf{a}_2$ . Consequently, the vector  $(n, m)$  is commonly used to classify carbon nanotubes. [5]



Figure 1: Snapshot sequence from an animation illustrating the unzipping of a carbon nanotube.

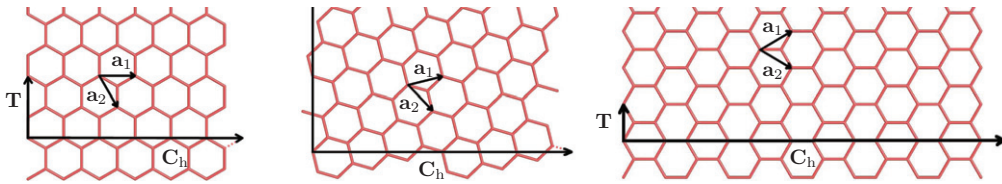


Figure 2: Definition of the wrapping and the base vectors in three different unzipped planar honeycomb structures. Left: (6,0), middle: (6,2), right: (6,6). See text for nomenclature.

In this common picture, the radius  $r_{\text{classical}}^{(n,m)}$  of a carbon nanotube is calculated by identifying the length of  $\mathbf{C}_h$  with the perimeter length of the tube:

$$2\pi r_{\text{classical}}^{(n,m)} = |\mathbf{C}_h| = a \sqrt{n^2 + nm + m^2}, \quad (1)$$

where  $a$  is the edge length in the lattice or the bond length between carbon atoms, respectively. The wrapping angle  $\theta_{\text{classical}}^{(n,m)}$  is defined to be the angle between  $\mathbf{C}_h$  and  $\mathbf{a}_1$ :

$$\cos \theta = \frac{\mathbf{C}_h \cdot \mathbf{a}_1}{|\mathbf{C}_h| |\mathbf{a}_1|} = \frac{2n + m}{2 \sqrt{n^2 + nm + m^2}}. \quad (2)$$

Although visualizations sometimes lead to premature assumptions, they are obviously and doubtlessly quite useful and instructive for the imagination and interpretation of scientific data, as Figs. 1 and 2 exhibit. Figure 1 shows snapshots from an animation made with the `animate`-package [9] for  $\text{\LaTeX}$ . The input picture sequence was created using the latest Atomistic Simulation Visualization software AViz [10, 11].

## 3. The polyhedral model and effect of correction terms

Comparing tubelike ground states of adsorbed polymers and carbon nanotubes, one first notes that the polymer does not crystallize in a honeycomb lattice, but rather in a triangular lattice. See Fig. 3 showing a triangular (3,0) tube, for example. However, this does not change much in the above described picture. As the lattices are dual in a sense, i.e., one can imagine the sites of the triangular lattice residing in the vacancies of the honeycomb lattice or centers of the hexagons, one can obviously use the same notation and calculation as introduced above. The only difference is that  $a$  has to be scaled by a factor of  $\sqrt{3}$ .

However when one compares numerical details, one notes almost immediately that the above described common approximation does not provide a suitable model to describe our computational results. To illustrate this, we present a comparison of radii in Fig. 4. The top row (upside-down solid triangles) shows the solutions of Eq. (1) for all  $n$

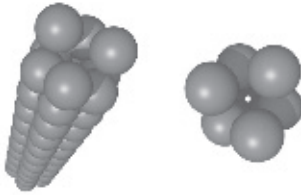


Figure 3: A triangular nanotube with  $(n, m) = (3, 0)$ , shown from different perspectives. See text for nomenclature.



Figure 4: Possible radii calculated with usual formula (solid, upside-down triangles) and radii of defect-free ground-state structures found in simulations (open triangles).

and  $m$  values corresponding to  $r_{\text{classical}}^{(n,m)} < 1.4$ . The bottom row (upright open triangles) represents radii where we find defect-free chiral ground states of polymer tubes in our simulations. Obviously, there is no apparent link between both sequences. We will illustrate (assuming that the bond length between monomers or atoms remains fixed) how the deviations can be explained using two simple examples. Consider first a triangular  $(3,0)$  tube as shown above in Fig. 3, i.e., a tube where three bonds and three monomers lie in a plane perpendicular to the tube center. With  $a = 1$ , one gets  $r_{\text{classical}}^{(3,0)} = 3/(2\pi)$ . However, the three bonds form a triangle where the sum of the edge lengths equals 3 and the radius of the circumcircle reads  $r_{\text{exact}}^{(3,0)} = \sqrt{3}/3$ . As a further example take the  $(3,3)$  triangular tube, where  $|C_n| = 3\sqrt{3}$  and hence  $r_{\text{classical}}^{(3,3)} = 3\sqrt{3}/(2\pi)$ . On the other hand the six corresponding bonds form, projected to a normal plane, a hexagon with edge length  $\cos(\pi/6)$ . The radius of the circumcircle equals the edge length in a hexagon and therefore  $r_{\text{exact}}^{(3,3)} = \cos(\pi/6)$ . In both examples, obviously  $r_{\text{classical}}^{(n,m)} \neq r_{\text{exact}}^{(n,m)}$ .

In fact, when zipping a two-dimensional discrete honeycomb structure, the geometry changes due to the introduced curvature. Such curved structures should hence be described by applying a suitable three-dimensional model rather than an effective two-dimensional one. For triangular tubes and under the assumption that the edge lengths remain fixed<sup>1</sup>, such a model is, for example, the polyhedral model introduced for the description of idealized boron nanotubes [13]. Calculations within this model lead to transcendental equations for both, the radius of the nanotubes and the chiral angle, which must be solved iteratively. In Fig. 5, we compare the radii of triangular nanotubes calculated using the classical and the polyhedral model as well as the difference for all  $n$  and  $m$ . In Fig. 5(a), where the values of the radii are ordered with respect to  $n$  and  $m$ , those differences do not seem to be of importance as the qualitative structure of the curve is the same for both models. But if one sorts the same data with respect to  $r$ , as

<sup>1</sup>This assumption does not necessarily hold in nature, though. See, for example [12].

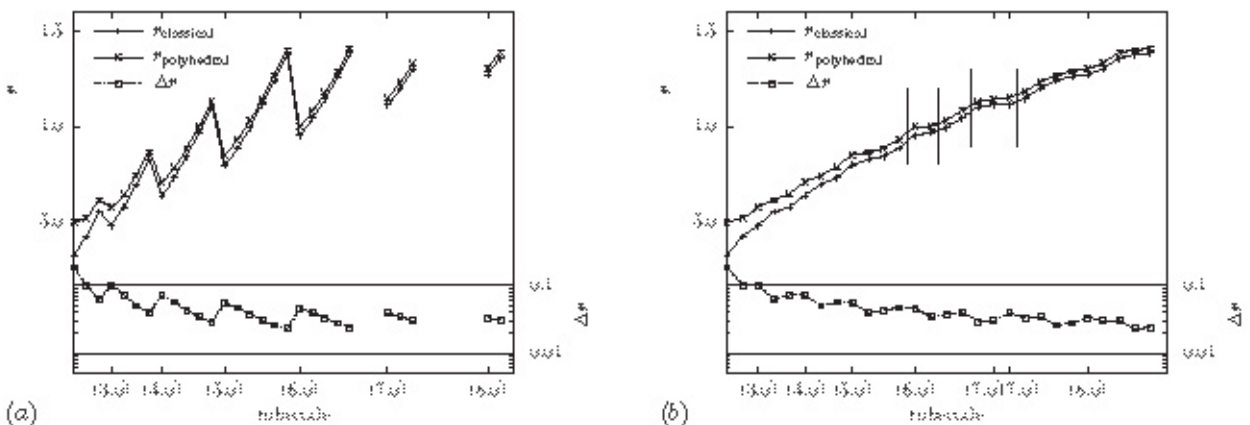


Figure 5: Comparison of radii of triangular nanotubes calculated in the classical and in the polyhedral model. (a) Data sorted with respect to growing  $n$ . Data points between  $(n, 0)$  and  $(n + 1, 0)$  correspond to  $(n, m)$  with  $m \in \{0 \dots n\}$ . (b) Data sorted with respect to  $r$ .

shown in Fig. 5(b), the effect of the deviations becomes apparent. As indicated exemplarily by the vertical dotted lines, there are intervals where the differences between the radii of two, in general completely different, nanotubes is smaller than the difference between the radii for the same tube calculated with the different models. Hence, one can not really resolve the link between radius and structure of nanotubes by using a simple planar ansatz.<sup>2</sup>

It should be mentioned that when expanding the relations for radius and chiral angle [13], the first term of the expansion is indeed the same term as one obtains when applying the planar model (cp. Eqs. (1) and (2)). However the higher order terms are relevant and must not be ignored at least in computational studies.<sup>3</sup>

#### 4. Structure of monolayer polymer tubes

If we apply the correct polyhedral model for triangular nanotubes, we find indeed a perfect match between calculated observables and those found in simulations, in contrast to the situation earlier depicted in Fig. 4. We show the results of both, calculation and results from simulations, in Table 1. In the second column, calculated radii using the polyhedral model [13] are given, in the following three columns simulational details can be found and in the last two columns we list the calculated wrapping angles using a suitable polyhedral model for carbon nanotubes<sup>4</sup> [14].

polyhedral polymer tube	Simulation on Cylinder surface ("2D")				Corresponding carbon nanotube	
	$r_{\text{exact}}^{(n,m)}$	$r_{\text{input}}$	output (Ground State) type	$\theta$ in °	$\theta$ in °	type
(2,1)	0.51962	0.477...0.532	3-helix	20.8...17.5	18.43	(2,1)
(3,0)	0.57735	0.553...0.574	(3,0)	0.0 ± 0.5	0.00	(3,0)
(2,2)	0.61237	0.585...0.617	(2,2)	31.3...29.6	30.00	(2,2)
(3,1)	0.64526	0.627...0.670	4-helix	13.9...12.6	13.57	(3,1)
(4,0)	0.70711	0.680...0.712	(4,0)	0.0 ± 0.5	0.00	(4,0)
(3,2)	0.74313	0.723...0.755	5-helix	23.8...22.7	23.33	(3,2)
(4,1)	0.78561	0.765...0.808	5-helix	11.0...10.2	10.72	(4,1)
(5,0)	0.85065	0.819...0.851	(5,0)	0.0 ± 0.6	0.00	(5,0)
(3,3)	0.86603	0.861	(3,3)	29.9 ± 0.4	30.00	(3,3)
(4,2)	0.88462	0.872...0.904	6-helix	19.2...18.3	19.01	(4,2)
(5,1)	0.93259	0.914...0.957	6-helix	9.0...8.4	8.84	(5,1)
(6,0)	1.00000	0.967...	(6,0)	0.0 ± 0.5	0.00	(6,0)
(4,3)	1.00188	...1.021	7-helix	26.2 ± 0.7	25.26	(4,3)
(5,2)	1.03116	1.031...1.052	7-helix	15.9...15.5	16.02	(5,2)
(6,1)	1.08319	1.063...1.106	7-helix	7.6...7.2	7.52	(6,1)
(4,4)	1.13152	1.106...1.127	(4,4)	30.3...30.0	30.00	(4,4)
(5,3)	1.14441	1.138	8-helix	21.7 ± 0.4	21.75	(5,3)
(7,0)	1.15238	1.148...1.169	(7,0)	0.0 ± 0.6	0.00	(7,0)
(6,2)	1.18076	1.169...1.201	8-helix	13.9...13.4	13.83	(6,2)
(7,1)	1.23600	1.212...1.254	8-helix	6.7...6.4	6.54	(7,1)
(5,4)	1.26887	1.244...1.276	9-helix	26.8...26.0	26.32	(5,4)
(6,3)	1.29090	1.286	9-helix	19.0 ± 0.5	19.07	(6,3)
(8,0)	1.30656	1.297...1.318	(8,0)	0.0 ± 0.6	0.00	(8,0)
(7,2)	1.33242	1.318...1.361	9-helix	12.2...11.8	12.17	(7,2)
(8,1)	1.39027	1.371...1.424	9-helix	5.8...5.6	5.79	(8,1)

Table 1: Comparison of calculated observables for nanotubes using polyhedral models and results from computer simulations of polymers on a cylinder surface. The rows are ordered with respect to  $r_{\text{exact}}^{(n,m)}$ .

In order to facilitate the simulations and to obtain more precise data, we adapted the model with respect to the given problem. In contrast to our recent study [1] we introduced flexible nonelastic bonds between monomers modeled by the FENE potential and changed the non-bonded Lennard-Jones potential such, that the equilibrium distances of both

<sup>2</sup>Additionally, the planar ansatz can lead to ambiguities as indicated by the the label for the (7,0) tube in Fig. 5(b). In fact, within that model, the radii for the (5,3) tube and the (7,0) tube are exactly the same.

<sup>3</sup>Just for the limiting cases  $m = 0$  and  $n = m$  the higher order terms in the calculation of the chiral angle vanish. The examples given above for the (3,0) and (3,3) tube are therefore correct.

<sup>4</sup>In contrast to the planar representation, there is no longer a trivial scaling between radii for triangular and honeycomb nanotubes when applying the respective polyhedral models. However, the wrapping angles are the same.

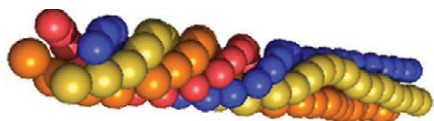


Figure 6: A ground-state conformation found in a general study of polymers adsorbed to ultrathin nanowires. The structure is composed of two competing regions with different chiralities.

interactions match. Furthermore we initialized the simulation with a configuration where all monomers have the same predetermined perpendicular distance to the nanowire and allowed only update moves which not change that distance. In practice, we simulated a flexible polymer on cylinder surfaces with more than one hundred different radii ( $r_{\text{input}}$ ) and searched for non-defective ground states, of which we measured the chiral angle  $\theta$ . On the one hand, we find the respective polymers tubes indeed for those radii calculated from the polyhedral model for triangular nanotubes (cp. columns two and three in Table 1), on the other hand we also measure exactly the wrapping angles which we calculate for carbon nanotubes (cp. columns five and six).

Hence, the ground states of monolayer polymers nanotubes forming at strongly attractive nanowires can be well described by the polyhedral model for idealized boron nanotubes and the sequence of wrapping angles when changing the radius of the polymer tube is exactly that calculated for carbon nanotubes. Our simulations are furthermore very precise, we can resolve that sequence even for tubes whose radii differ by  $< 1\%$  (cp.  $r_{\text{exact}}^{(6,0)}$  and  $r_{\text{exact}}^{(4,3)}$  or  $r_{\text{exact}}^{(5,3)}$  and  $r_{\text{exact}}^{(7,0)}$ ), which was not possible before.

We can also explain specific results from our general study. Figure 6 shows a low-energy conformation with tube radius  $0.6 < r < 0.7$  found for the originally used polymer–wire model [1]. It shows two competing regions forming a helix with four strands and a (2,2) structure, respectively. For the first one we measure a wrapping angle  $\theta \approx 14^\circ$ . Looking up in Table 1 we find that that part corresponds to a (3,1) tube and that this is a direct neighbor of the (2,2) tube with respect to the possible discrete radii for  $(n, m)$  tubes. Indeed, it is plausible, that there is competition between these structure for radii that do not match exactly any  $r_{\text{exact}}^{(n,m)}$ .

## 5. Summary

In this paper we argued that polyhedral models for nanotubes are useful for the description of respective structures in computational studies. The corrections introduced by those models compared to the commonly used pictures are in general not negligible (see also a recent study on the effect of chirality on nanotube vibrations [15]). In particular, the polyhedral model for boron nanotubes reflects the findings of monolayer polymer nanotube structures found earlier. The sequence of chiral angles of polymer nanotubes with different radii is the same as for carbon nanotubes and provides the link between those structures.

*Acknowledgments.* The authors would like to thank P. Pine and S. Srebnik from the Technion Haifa for valuable discussions on nanotubes and adsorption of polymers at nanotubes. This project is supported by the Jülich/Aachen/Haifa Umbrella program under Grants No. SIM6 and No. HPC\_2. Supercomputer time is provided by the Forschungszentrum Jülich under Projects No. jiff39 and No. jiff43.

- [1] T. Vogel, M. Bachmann, Phys. Rev. Lett. 104 (2010) 198302.
- [2] T. Vogel, M. Bachmann, Phys. Procedia 4 (2010) 161.
- [3] T. Vogel, M. Bachmann, Comp. Phys. Comm., *in press*. doi:10.1016/j.cpc.2010.11.007.
- [4] J. W. G. Wilder, L. C. Venema, A. G. Rinzler, R. E. Smalley, C. Dekker, Nature 39 (1998) 59.
- [5] M. S. Dresselhaus, G. Dresselhaus, P. Avouris (Eds.), Carbon Nanotubes: Synthesis, Structure, Properties, and Applications, Vol. 80 of Topics in Applied Physics, Springer, Heidelberg, 2001.
- [6] T. Mutat, M. Sheintuch, J. Adler, J. Chem. Phys. 134 (2011) 044908.
- [7] P. Pine, Y. Yaish, J. Adler, Simulation and vibrational analysis of thermal oscillations of single-walled carbon nanotubes, Phys. Rev. B, *to appear*.
- [8] T. Vogel, T. Mutat, J. Adler, M. Bachmann, Morphological similarities of carbon nanotubes and polymers adsorbed on nanowires, *preprint*.
- [9] A. Grahn, <http://www.tug.org/texlive/Contents/live/texmf-dist/doc/latex/animate/animate.pdf>.
- [10] <http://phycomp.technion.ac.il/~newaviz/>.
- [11] J. Adler, Y. Koenka, A. Silverman, Adventures in carbon visualization with AViz, *this issue*.
- [12] M. Budyka, T. Zyubina, A. Ryabenko, S. Lin, A. Mebel, Chem. Phys. Lett. 407 (2005) 266.
- [13] R. K. F. Lee, B. J. Cox, J. M. Hill, J. Phys. A: Math. Theor. 42 (2009) 065204.
- [14] B. J. Cox, J. M. Hill, Carbon 45 (2007) 1453.
- [15] P. Pine, Y. Yaish, J. Adler, *in preparation*.